A Slotted Circular Patch Antenna with Wideband Filtering Characteristics

Manisha Kahar, Mrinal Kanti Mandal
Department of Electronics & Electrical Communication Engineering
Indian Institute of Technology Kharagpur
Kharagpur, India
manishakahar@gmail.com, mkmandal@ieee.org

***Abstract*—A circular microstrip patch antenna is fed at its center to simultaneously excite the fundamental TM_{01} and higher order TM_{0n} modes resulting in omni-directional azimuthal coverage. Two annular ring slots are etched on the circular patch to couple the first three resonating modes. A method is described to control the coupling among the modes, which determine the bandwidth of the antenna and provides filtering characteristics. A prototype is fabricated for X-band application. It provides 28% 10 dB impedance bandwidth at 10.2 GHz. Gain variation is within 1% of 7dBi over the entire passband. The out of band suppression is better than 22 dB.**

***Keywords*—circular patch, filtering antenna, TM_{0n} mode.**

I. Introduction

The TM_{01} mode of circular microstrip patch antennas is widely used for its omni-directional radiation patterns [1], [2] which ensures signal coverage over a large angle. It finds extensive applications in WLANs and vehicle telematics. In a communication system, a band pass filter (BPF) is always used after the antenna. Thus, a filtering antenna can reduce insertion loss, system cost, and size of the overall system. Many omni-directional filtering antennas have been explored [3]–[5]. They are realized either using filter synthesis concept with radiator as the last resonator [3] or some ground plane perturbation [5]. Here the antenna efficiency is sacrificed by the insertion loss of the filtering unit preceding the radiator.

In this paper, a circular microstrip patch antenna is fed at its center without any ground plane deformation to excite the TM_{0n} modes which provide quasi-omni directional radiation patterns over a wide bandwidth. It is shown that intermodal coupling among the first three modes can be utilized to control the impedance bandwidth of the antenna. The filtering antenna provides radiation nulls at band edges with sufficient band rejection. Working principle of the antenna is explained with the help of full wave simulations using ANSYS HFSS. The ground plane size is selected to be 10 % [1] more than the circular patch diameter but satisfactory performance is maintained even with ground plane size 100 % more than the circular patch.

II. Antenna Design and Analysis

Fig. 1(a) shows a circular patch antenna. The antenna is designed on a Roger RO4003C substrate with relative permittivity $\varepsilon_r = 3.55$, thickness $h = 0.813$ mm, and loss tangent = 0.0027. Radius of the circular patch $R_p = 22.5$ mm and that of the ground plane is R_g = 25 mm. Fig. 1(b) shows the corresponding $|S_{11}|$. Three dips are due to TM_{01}, TM_{02} and TM_{03} modes. At these frequencies, the input impedance for the circular patch is high because of strong electric field and weak magnetic field at the patch centre resulting in poor matching. The surface current distribution corresponding to the excited modes are shown in Fig. 2(a). It is observed that there are two current minima circles corresponding to the TM_{03} mode at radius $R_1 = 9.5$ mm and $R_2 = 16$ mm. These minima circles are however not the current minima circle for the TM_{02} or TM_{01} modes. So, if slots are etched along the current minima circles of the TM_{03} mode, the mode characteristics remain unaffected because the

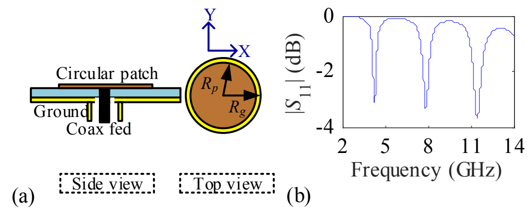

Fig. 1. (a) A centre fed circular patch and (b) its $|S_{11}|$ response.

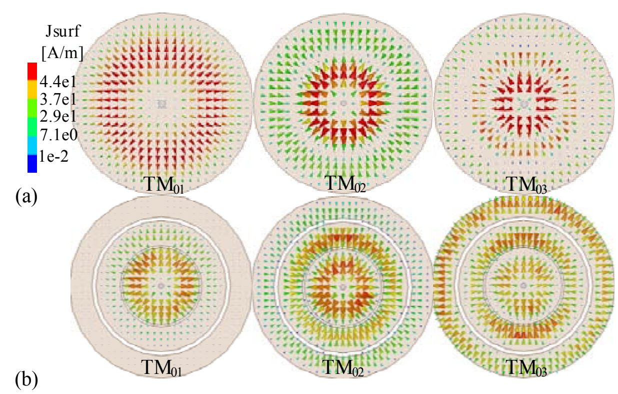

Fig. 2. Vector surface current distribution on the centre fed circular patch antenna for TM_{01}, TM_{02} and TM_{03} modes (a) without slot (b) with slot.

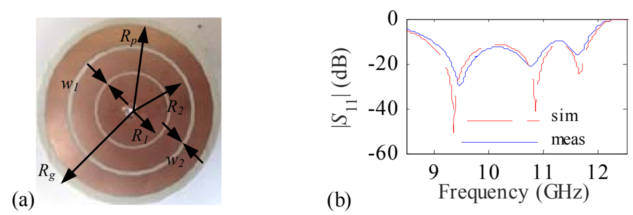

Fig. 3. (a) Fabricated slotted center fed circular patch antenna and (b) its measured and simulated $|S_{11}|$ responses with $R_g = 25$, $R_p = 22.5$, $R_1 = 9.5$, $R_2 = 16$, $w_1 = 0.5$, $w_2 = 1$, (unit: mm).

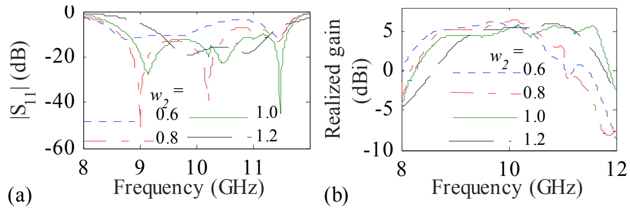

Fig. 4. (a) Bandwidth control using mode coupling and (b) realized gain vs. frequency in main beam direction.

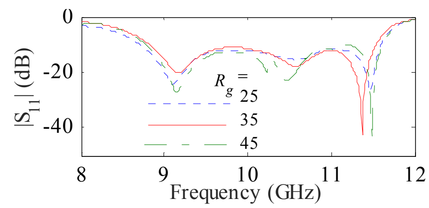

Fig. 5. $|S_{11}|$ response with variation in ground plane size R_g (in mm).

annular ring is analogous to an open-circuit plane for the TM_{03} mode which is understood from Fig. 2(b) where the slots are observed to squeeze the first two modes towards the patch centre without changing the field pattern. So the effective radiating area for these modes decrease resulting in upshift of corresponding resonant frequencies. The resonant frequency of the TM_{03} mode does not shift. So, the TM_{01} and TM_{02} modes gets coupled to it resulting in larger bandwidth. The fabricated antenna with two slots is shown in Fig. 3(a). Slots widths w_1 and w_2 are optimized as 0.5 mm and 1 mm, respectively, for maximum input impedance bandwidth. The simulated and measured $|S_{11}|$ response is shown in Fig. 3(b) for R_g = 25 mm.

III. Filtering Property

Bandwidth control by coupling between the first two modes, TM_{01} and TM_{02} is done by w_1. Similarly, coupling between TM_{03} mode with the pre-coupled TM_{01} and TM_{02} modes is controlled by w_2. Fig. 4(a) shows the bandwidth variation with w_2 when w_1 = 0.5 mm. Similar variation is observed when w_1 is changed keeping w_2 fixed. For very small w_2 below 0.8 mm, the three modes are strongly coupled but not matched. So, their individual poles are not prominent and overall bandwidth is small. With increase in w_2 up to 1 mm, the poles become clearly visible and the bandwidth increases. With further increase in w_2 above 1 mm, the coupling between the first two modes with that of the third becomes weaker and bandwidth again decreases. In this case, the TM_{03} mode no longer couples to the pre-coupled TM_{01} and TM_{02} modes. At this stage, the bandwidth may be controlled by w_1 only. This is trivial as the bandwidth from coupled TM_{01} and TM_{02} mode is less than that of the bandwidth from coupled TM_{01}, TM_{02} and TM_{03} modes and is not shown here.

The gain versus frequency plot in the direction of main beam with change in w_2 is shown in Fig. 4 (b). These plots also ascertain the controllable gain bandwidth by means of coupling between the modes as discussed above. There are the two radiation zeroes for w_2 = 1 mm at the pass band edges which gives a BPF like characteristics to the antenna. As there are no resonant frequency modes below the TM_{01} mode, the gain is supressed at the lower stop band frequency. The ring slots

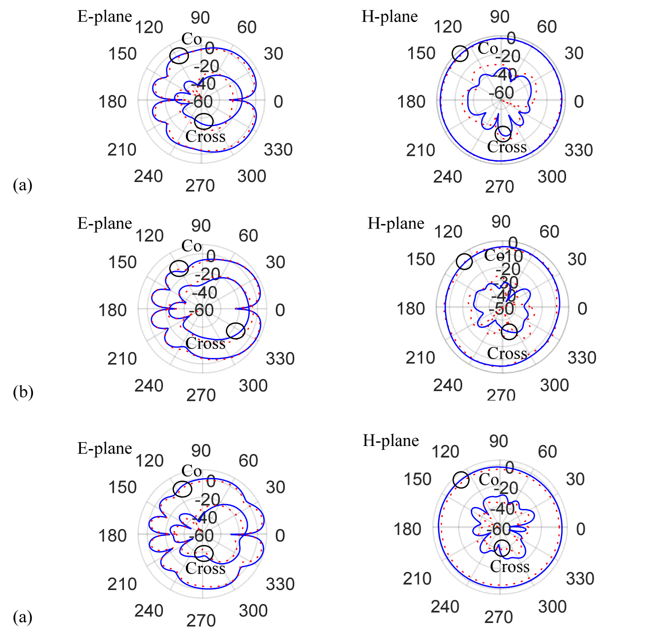

Fig. 6. Gain patterns at (a) 9.15 GHz, (b) 10.48 GHz and (c) 11.49 GHz (solid line: simulated data, dotted line:measured) .

upshift TM_{04} without affecting TM_{03} mode, thus providing upper stopband of the filtering antenna. Next the effect of finite ground plane is observed by varying ground plane radius, R_g from 25 mm to 45 mm in Fig. 5. No significant change is observed in bandwidth.

The measured and simulated E-plane (*XZ*-plane) and H-plane (*XY*-plane) gain patterns are shown in Fig. 6 at three dips of $|S_{11}|$. These dips at 9.15 GHz, 10.48 GHz and 11.49 GHz corresponds to the TM_{01}, TM_{02} and TM_{03} modes. Since the field orientation is similar for all these three modes, quasi-omni directional property is maintained with 20 dB cross polarization suppression over the whole impedance bandwidth. The main beam direction is always at $\theta = 25°$.

IV. Conclusion

A circular microstrip patch antenna with annular slots is presented with quasi-omni directional radiation patterns and wide band filtering characteristics over the whole impedance bandwidth. It is suitable for vehicle telematics applications.

References

[1] L. Economou and R. J. Langley, "Patch antenna equivalent to simple monopole," *Electronics Lett.*, vol. 33, no. 9, pp. 727 – 729, 24 Apr. 1997..

[2] A. Al-Zoubi, F. Yang and A. Kishk, "A broadband center-fed circular patch-ring antenna with a monopole like radiation pattern," *IEEE Trans. Antennas Propag.*, vol. 57, no. 3, pp. 789 – 792, Mar. 2009.

[3] C.-T. Chuang and S.-J. Chung, "Synthesis and design of a new printed filtering antenna," *IEEE Trans. Antennas Propag.*, vol. 59, no. 3,pp. 1036 – 1042, Mar. 2011.

[4] M. C. Tang, Y. Chen, and R. W. Ziolkowski, "Experimentally validated, planar, wideband, electrically small, monopole antennas based on capacitively loaded loop resonators," *IEEE Trans. Antennas Propag.*, vol. 64,no. 8, pp. 3353 – 3360, Aug. 2016.

[5] Y. Zhang, X. Y. Zhang and Y. Pan, "Low-profile planar filtering dipole antenna with omnidirectional radiation pattern," *IEEE Trans. Antennas Propag.*, vol. 66, no. 3, pp. 1124-1132, Mar. 2018.